Solid-state light-emitting electrochemical cells employing phosphor-sensitized fluorescence

Hai-Ching Su,*[a] You-Heng Lin,[b] Chih-Hao Chang,[b] Hao-Wu Lin,[b] Chung-Chih Wu,[b] Fu-Chuan Fang,[c] Hsiao-Fan Chen[c] and Ken-Tsung Wong[c]

Received 16th February 2010, Accepted 14th April 2010
First published as an Advance Article on the web 2nd June 2010
DOI: 10.1039/c0jm00429d

We report highly efficient phosphor-sensitized solid-state light-emitting electrochemical cells (LECs) utilizing a phosphorescent cationic iridium complex $[Ir(dFppy)_2(SB)]^+(PF_6^-)$ as the host and a fluorescent cationic dye (R6G) as the guest. Photophysical studies show that R6G retains a high photoluminescence quantum yield (PLQY) in highly polar media, revealing its suitable use as an emitting guest in an ionic host matrix. Such solid-state LECs achieve quantum efficiency (cd A^{-1}) efficiency, and power efficiency up to 5.5% photon/electron, 19 cd A^{-1} and 21.3 lm W^{-1}, respectively. The device quantum efficiency achieved is among the highest reported for fluorescent LECs and is higher than one would expect from the PLQY of the R6G fluorescent dye in the host film, thus indicating that phosphor-sensitization is useful for achieving highly efficient fluorescent LECs. Moreover, using narrow-band fluorescent emitters, such as R6G (FWHM, ~50 nm), is effective in improving the color saturation of solid-state LECs based on cationic complexes.

Introduction

Solid-state light-emitting electrochemical cells (LECs) possess several advantages over conventional organic light-emitting diodes (OLEDs). In LECs, electrochemically doped regions induced by spatially separated ions under a bias form ohmic contacts with electrodes, giving balanced carrier injection, low operating voltages and consequently high power efficiencies.[1,2] As such, LECs generally require only a single emissive layer, which can be easily processed from solutions, and can conveniently use air-stable electrodes, while OLEDs typically require more sophisticated multilayer structures and low-work-function cathodes.[3] Compared with conventional polymer LECs, which are usually composed of an emissive conjugated polymer, a salt and an ion-conducting polymer,[1,2] LECs based on cationic transition metal complexes show several further advantages and have attracted much attention in recent years.[4–15] In such devices, no ion-conducting material is needed since these metal complexes are intrinsically ionic. Furthermore, higher electroluminescent (EL) efficiencies are expected, due to the phosphorescent nature of the metal complexes.

As in OLEDs, the host–guest approach, *i.e.* spatially dispersing the emitting guest into a matrix complex (host), had been reported to be an effective way to tune the emission color or to improve the emission efficiency of solid-state LECs based on cationic transition metal complexes.[11,16] Thus far, all host–guest LECs based on previously reported cationic complexes were implemented by doping the phosphorescent cationic complexes (guest) into the host cationic complexes, which were also phosphorescent. Nevertheless, doping fluorescent guests into phosphorescent hosts may be an alterative way to achieve efficient/color-tunable host–guest LECs, since, in conventional OLED technologies, phosphor-sensitization had been proved to be useful in raising the efficiency of fluorescent OLEDs to similar levels to phosphorescent OLEDs. In phosphor-sensitized fluorescence, the heavy-metal center of the phosphorescent host mediates rapid inter-system crossing for efficient intramolecular singlet-to-triplet energy transfer, and thus subsequent effective Förster energy transfer[17] from triplet excitons of the phosphor host to singlet excitons of the fluorophore guest, harvesting both singlet and triplet excitons in hosts.[18,19] The shorter excited-state lifetimes of fluorescent guests could also possibly reduce the triplet–triplet annihilation issues in purely phosphorescent devices, which is associated with high triplet populations induced by long excited-state lifetimes of triplet excitons. As a result, device efficiencies of phosphor-sensitized fluorescent OLEDs could approach those of phosphorescent OLEDs.[18,19] Despite its successful use in OLEDs, however, up to date, there is no demonstration or report of employing phosphor-sensitized fluorescence in host–guest solid-state LECs based on cationic transition metal complexes. In this work, we report investigations on Ir-complex-based solid-state LECs utilizing phosphor-sensitized fluorescence.[18,19]

Results and discussion

PL and photophysical studies of phosphor sensitization

The chemical structures of the host and guest materials used in this study are shown in Fig. 1. The previously reported green-emitting cationic Ir complex $[Ir(dFppy)_2(SB)]^+(PF_6^-)$ (where

[a]*Institute of Lighting and Energy Photonics, National Chiao Tung University, Tainan, Taiwan, 71150, Republic of China. E-mail: haichingsu@mail.nctu.edu.tw; Fax: +886-6-3032535; Tel: +886-6-3032121-57792*
[b]*Department of Electrical Engineering, Graduate Institute of Photonics and Optoelectronics, Graduate Institute of Electronics Engineering, National Taiwan University, Taipei, Taiwan, 10617, Republic of China*
[c]*Department of Chemistry, National Taiwan University, Taipei, Taiwan, 10617, Republic of China*

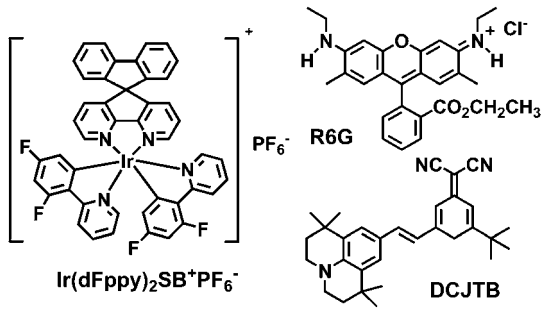

Fig. 1 The molecular structures of $[Ir(dFppy)_2(SB)]^+(PF_6^-)$, R6G and DCJTB.

dFppy is 2-(2,4-difluorophenyl)pyridine and SB is 4,5-diaza-9,9′-spirobifluorene)[10,11] was used as the phosphorescent host in this study. Neat films of the host exhibit green photoluminescence (PL) centered at 535 nm. The host shows relatively high PL quantum yields (PLQYs, ~31%), even in neat films, due to the superior steric hindrance provided by the bulky diazaspirobifluorene-based (SB) auxiliary ligand.[10] Rather efficient solid-state LECs had been achieved using this cationic Ir complex.[11] Meanwhile, two types of fluorescent dyes, a neutral organic fluorescent dye 4-(dicyanomethylene)-2-*t*-butyl-6-(1,1,7,7-tetramethyljulolidyl-9-enyl)-4*H*-pyran (DCJTB) and a cationic fluorescent dye (Rhodamine 6G (R6G)), were used as the fluorescent guests. Both guests show intense absorption bands near the emission band of the host and thus host–guest energy transfer is expected to be feasible.

Fig. 2(a) and 2(b) show the PL spectra of the $[Ir(dFppy)_2(SB)]^+(PF_6^-)$ host films doped with various concentrations of R6G and DCJTB guests, respectively. Neat films of the host exhibit green PL centering at 535 nm, where the R6G and DCJTB guest show intense absorption bands (Fig. 2). Thus, effective host–guest energy transfer is expected (calculated Förster radius = 4.33 nm for $[Ir(dFppy)_2(SB)]^+(PF_6^-)$/R6G host–guest system, 4.28 nm for $[Ir(dFppy)_2(SB)]^+(PF_6^-)$/DCJTB host–guest system). Dominant guest emission, even at low doping concentrations, indicates efficient energy transfer in both host–guest systems. The PL spectrum of $[Ir(dFppy)_2(SB)]^+(PF_6^-)$ is broad (FWHM, ~100 nm) due to its metal-to-ligand charge transfer (MLCT) nature. In particular, the FWHM of the PL spectrum reduces to ~50 nm when R6G is added as guest with a doping concentration greater than 0.05 wt%. Further increasing the doping concentration leads to slight bathochromic shift associated with an enhanced molecular polarization effect,[20] but the FWHM of the PL spectrum remains similarly small. Thus, with R6G guests, not only si the emission color tuned, but also the color becomes much more saturated.

The photophysical properties of R6G and DCJTB in host matrices of different polarities were further characterized.

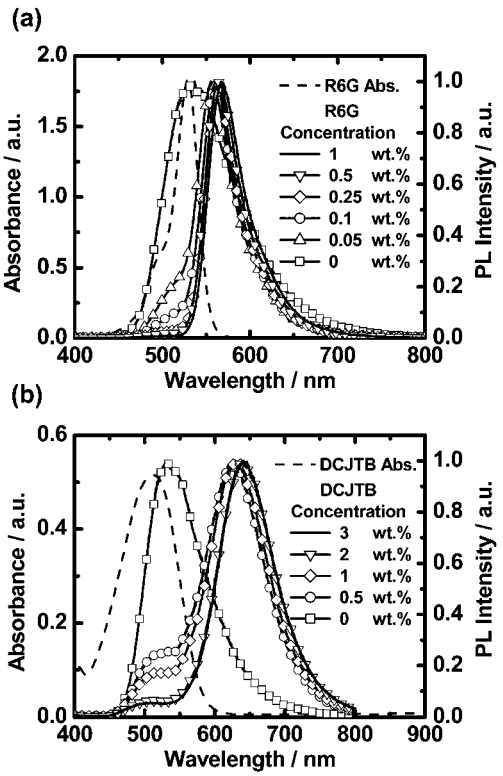

Fig. 2 (a) PL spectra of $[Ir(dFppy)_2(SB)]^+(PF_6^-)$ films doped with various R6G concentrations and the absorption spectrum of R6G in 10^{-5} M MeOH, and (b) PL spectra of $[Ir(dFppy)_2(SB)]^+(PF_6^-)$ films doped with various DCJTB concentrations and the absorption spectrum of DCJTB in 10^{-5} M CH_2Cl_2.

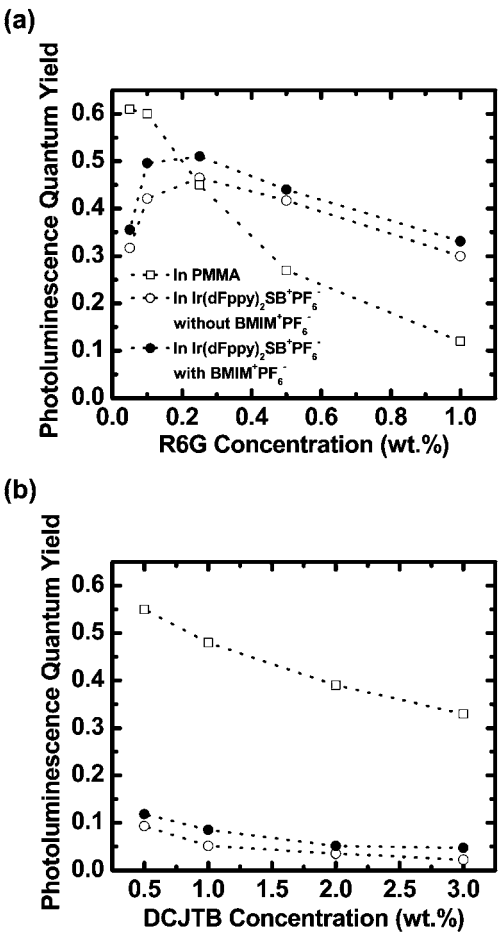

Fig. 3 Doping concentration-dependent photoluminescence quantum yields of (a) R6G, and (b) DCJTB in host films of PMMA, $[Ir(dFppy)_2(SB)]^+(PF_6^-)$, and $[Ir(dFppy)_2(SB)]^+(PF_6^-)$/$BMIM^+(PF_6^-)$.

Concentration-dependent PLQYs of R6G and DCJTB doped in PMMA films, in $[Ir(dFppy)_2(SB)]^+(PF_6^-)$ films, and in $[Ir(dFppy)_2(SB)]^+(PF_6^-)$/$BMIM^+(PF_6^-)$ (where BMIM is 1-butyl-3-methylimidazolium) films are depicted in Fig. 3(a) and Fig. 3(b), respectively. The ionic liquid $[BMIM^+(PF_6)^-]$ was added to enhance the ionic conductivity of thin films and consequently to shorten the LEC response times.[8] Meanwhile, excited-state lifetimes for R6G-doped films (at 600 nm) and DCJTB-doped films (650 nm) as a function of doping concentrations in various host films were also characterized and are depicted in Fig. 4(a) and 4(b), respectively. Excited-state lifetimes on the order of nanoseconds for both guests in $[Ir(dFppy)_2(SB)]^+(PF_6^-)$ or $[Ir(dFppy)_2(SB)]^+(PF_6^-)$/$[BMIM^+(PF_6)^-]$ hosts again confirm the phosphor-sensitized fluorescent emission.

As shown in Fig. 3(a) and 3(b), both R6G and DCJTB possess high PLQYs of ~60% in the non-ionic PMMA host matrix at low doping concentrations. In the ionic $[Ir(dFppy)_2(SB)]^+(PF_6^-)$ or $[Ir(dFppy)_2(SB)]^+(PF_6^-)$/$[BMIM^+(PF_6)^-]$ host matrices, R6G retains high PLQYs of ~40–50% over the concentration range tested, which is indeed enhanced over the PLQY (~31%) of the $[Ir(dFppy)_2(SB)]^+(PF_6^-)$ neat film. In contrast, when doped into the ionic $[Ir(dFppy)_2(SB)]^+(PF_6^-)$ or $[Ir(dFppy)_2(SB)]^+(PF_6^-)$/$[BMIM^+(PF_6)^-]$ host matrices, PLQYs of DCJTB have dropped significantly down to ≤10%, even at low doping concentrations (which is even lower than the PLQY of the $[Ir(dFppy)_2(SB)]^+(PF_6^-)$ neat film). Such differences in the photophysical properties of DCJTB and R6G may be associated with their different responses in media of different polarities, and thus we further characterized their PLQYs and excited-state lifetimes in two solvents of different polarity, MeOH (more polar) and CH_2Cl_2 (less polar). These results are summarized in Table 1. As shown in Table 1, DCJTB exhibits significantly lowered PLQYs and shortened excited-state lifetimes in more polar MeOH than in CH_2Cl_2. Photophysical transitions of DCJTB are of significant intramolecular charge-transfer nature and thus the substantial decrease of its PLQY in highly polar solvents (or solid-state host matrices) is mostly due to strong interactions between highly polarized excited-state chromophores and surrounding molecules.

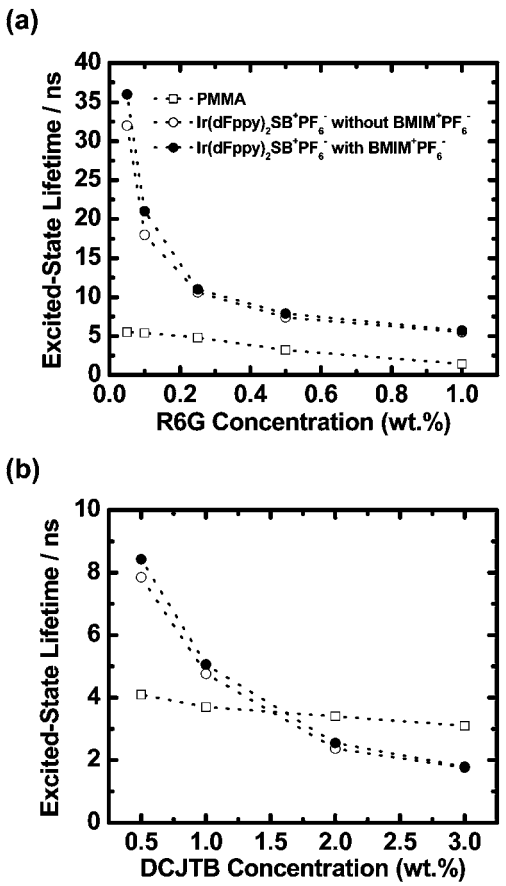

Fig. 4 Doping concentration-dependent excited-state lifetimes of (a) R6G (at 600 nm), and (b) DCJTB (at 650 nm) in host films of PMMA, $[Ir(dFppy)_2(SB)]^+(PF_6^-)$, and $[Ir(dFppy)_2(SB)]^+(PF_6^-)$/$BMIM^+(PF_6^-)$.

Table 1 The photophysical properties for R6G and DCJTB in CH_2Cl_2 and MeOH

	PLQY (%)		Lifetime/ns	
	CH_2Cl_2	MeOH	CH_2Cl_2	MeOH
R6G	63	89	4.4	4.8
DCJTB	57	12	2.6	0.6

On the other hand, R6G shows lower PLQYs and shorter excited-state lifetimes in less polar CH_2Cl_2 than in MeOH. R6G shows a high PLQY of 0.89 in highly polar methanol (MeOH), but a lower PLQY of 0.63 in less polar dichloromethane (CH_2Cl_2). Similar phenomena were also observed when dispersing R6G in solid-state hosts of different polarities. In Fig. 3(a), one notices that R6G exhibits higher PLQYs in an $[Ir(dFppy)_2(SB)]^+(PF_6^-)$ or $[Ir(dFppy)_2(SB)]^+(PF_6^-)$/$[BMIM^+(PF_6)^-]$ film than in a PMMA film for doping concentration of 0.25~1.0 wt.%; while in Fig. 4(a), one notices excited-state lifetimes are shortened for the R6G-doped PMMA than for R6G-doped $[Ir(dFppy)_2(SB)]^+(PF_6^-)$ or $[Ir(dFppy)_2(SB)]^+(PF_6^-)$/$[BMIM^+(PF_6)^-]$. In particular, with the addition of $BMIM^+(PF_6^-)$ (19 wt%) in the cationic host, even higher PLQYs and longer excited-state lifetimes occur in the host–guest systems, perhaps due to dilution effects and reduced interchromophore quenching.[11] Lower PLQYs and shorter excited-state lifetimes for R6G in less polar solvents (hosts) is mostly associated with charge-transfer interactions (deactivation processes) between excited-state cations and associated anions (Cl^-), since the anions cannot be fully dissociated with the cations in less polar solvents (hosts).[21] In view of the above results, ionic fluorescent dyes like R6G appear more suitable than neutral organic dyes like DCJTB for use as guests in phosphor-sensitized fluorescent LECs, in which host materials are ionic and polar.

It is noted that the PLQY of R6G-doped PMMA increases and yet R6G-doped $[Ir(dFppy)_2(SB)]^+(PF_6^-)$ decreases when the doping concentration decreases from 0.25 to 0.05 wt% (Fig. 3(a)). In R6G-doped PMMA, the increase of the PLQY with a decrease of the doping concentration is due to reduced self-quenching, which is accompanied by increased excited-state lifetimes (Fig. 4(a)). R6G-doped $[Ir(dFppy)_2(SB)]^+(PF_6^-)$ also shows a similar increasing trend when reducing the doping concentration from 1.0 to 0.25 wt%, but an opposite trend is observed for further reducing the doping concentration. Energy

transfer from $[Ir(dFppy)_2(SB)]^+(PF_6^-)$ to R6G becomes less complete (see residual host emission in Fig. 2) at low doping concentrations (<0.25 wt%). Since the PLQY of the $[Ir(dFppy)_2(SB)]^+(PF_6^-)$ neat film (0.31) is lower than that of diluted R6G in $[Ir(dFppy)_2(SB)]^+(PF_6^-)$, incomplete energy transfer leads to a mixture of host and guest emission and thus lowered PLQYs. Incomplete host–guest energy transfer is also reflected in the much-lengthened excited-state lifetimes of R6G-doped $[Ir(dFppy)_2(SB)]^+(PF_6^-)$ at low concentrations (*e.g.* at the concentration of 0.05 wt%, Fig. 4(a)). At low doping levels, the small amount of guest molecules is not efficient enough for deactivating excitons on the excited (phosphorescent) cationic complex host, thus resulting in longer observed lifetimes.

EL characteristics of phosphor-sensitized LECs

Phosphor-sensitized fluorescent LECs with various R6G doping concentrations exhibited similar time-dependent EL characteristics under constant-bias operation. Fig. 5(a) shows the time-dependent brightness and current density under constant biases of 2.7–2.9 V for the phosphor-sensitized LEC with host ($[Ir(dFppy)_2(SB)]^+(PF_6^-)$), guest (R6G) and $BMIM^+(PF_6^-)$ concentrations of 80.95, 0.05 and 19 wt%, respectively. After the bias was applied, the current first increased and then stayed rather constant. On the other hand, the brightness first increased with the current and reached the maxima of 12, 48 and 149 cd m^{-2} at ~0.5 h under biases of 2.7, 2.8 and 2.9 V, respectively. The brightness then dropped with time with a rate depending on the bias voltage (or current). The lifetime of the phosphor-sensitized LECs, defined as the time it takes for the brightness of the device to decay from the maximum to half of the maximum under a constant bias of 2.9 V is 2.8 h. Slight reduction of the applied bias by 0.1 V led to improved device stability and thus lengthened device lifetimes (5.2 h). However, the host-only devices under 2.9 V and 2.8 V driving exhibited lifetimes of 6.7 and 12 h, respectively.[10] Further examination of the EL characteristics of devices is required to clarify the deteriorated stability of the phosphor-sensitized LECs. Corresponding time-dependent EQEs and power efficiencies of the same device are shown in Fig. 5(b). When a forward bias was just applied, the EQE was rather low due to poor carrier injection. During the formation of the p- and n-type regions near electrodes, the capability of carrier injection was improved and the EQE thus rose rapidly. The peak EQE (cd A^{-1}) and peak power efficiencies at 2.7, 2.8 and 2.9 V are (5.3%, 18.2 cd A^{-1}, 21.2 lm W^{-1}), (5.5%, 19.0 cd A^{-1}, 21.3 lm W^{-1}) and (5.5%, 18.8 cd A^{-1}, 20.3 lm W^{-1}), respectively. The drop of efficiencies and brightnesses after reaching the peak value, as commonly seen in solid-state LECs,[4–15] may be associated with a few factors. Before the current reaches a steady value, the carrier recombination zone may keep moving closer to one electrode due to discrepancy in electron and hole mobilities, which would induce exciton quenching. Further, the decrease in brightnesses/efficiencies under a constant bias may be rationally associated with the degradation of the emissive material during the LEC operation.[22–25] It is noted that the decreasing rates of brightness/EQEs of the phosphor-sensitized LECs are higher than those of host-only devices before reaching steady device currents.[10] However, the decreasing rates of brightness/EQEs of phosphor-sensitized and host-only LECs are similar after the steady device currents are reached.[10] Thus, shorter device lifetimes of phosphor-sensitized LECs compared to the host-only devices may be associated with the dynamic carrier recombination zone since the carrier balance would be altered by guest doping. Further studies of appropriate host–guest combinations may be helpful to improve the device stability of phosphor-sensitized LECs.

The EL spectra of phosphor-sensitized LECs with various R6G concentrations are shown in Fig. 6. EL spectra are basically similar to PL spectra of the emission layers, indicating similar emission mechanisms. The FWHM of the EL spectra drops from 70 to 45 nm as the R6G concentration increases from 0.05 to 0.2 wt%. At lower R6G concentrations, the EL spectra are composed of both host and guest emission due to incomplete

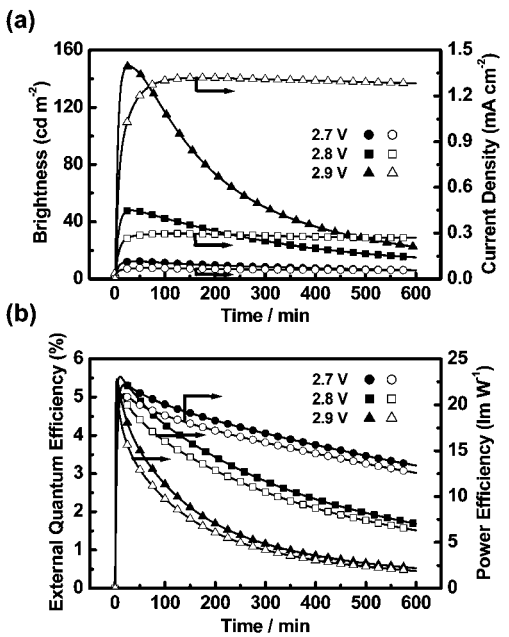

Fig. 5 (a) Brightness (solid symbols) and current density (open symbols) and (b) external quantum efficiency (solid symbols) and power efficiency (open symbols) as a function of time under a constant bias voltage of 2.7–2.9 V for the LEC with $[Ir(dFppy)_2(SB)]^+(PF_6^-)$, R6G and $BMIM^+(PF_6^-)$ concentrations of 80.9, 0.1 and 19 wt%, respectively.

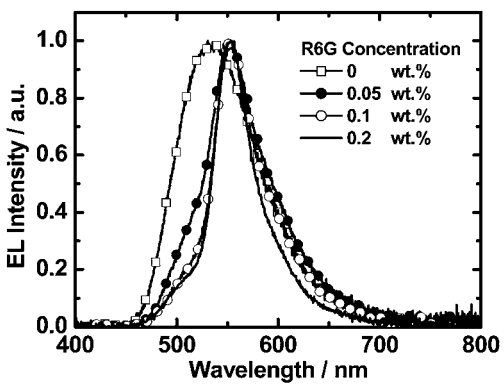

Fig. 6 EL spectra (at 2.7 V) for phosphor-sensitized LECs with various R6G concentrations.

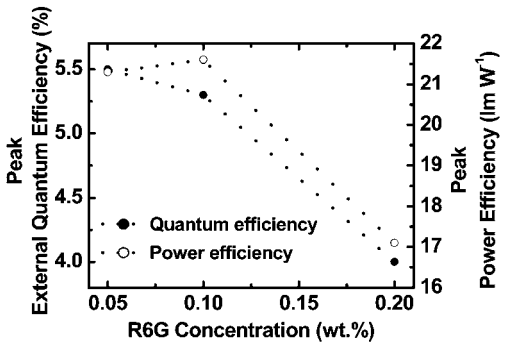

Fig. 7 Peak external quantum efficiencies and peak power efficiencies (at current densities <0.2 mA cm^{-2}) of phosphor-sensitized LECs as a function of the R6G concentration.

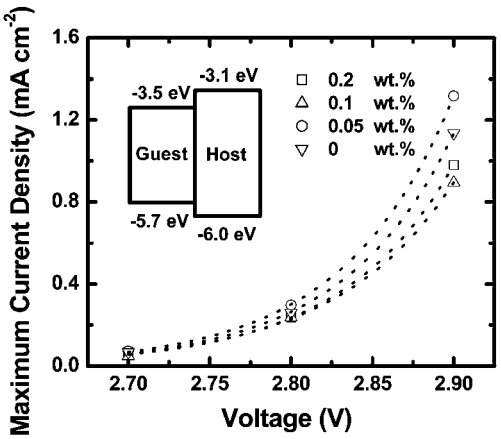

Fig. 8 Maximum current density *vs.* voltage characteristics for LECs with various R6G concentrations. Inset: the energy level diagram of the host and guest molecules.

host–guest energy transfer and the FWHM of the EL spectra are thus broader. As the doping concentration increases, efficient energy transfer suppresses the host emission and the EL spectra resemble their PL spectra (Fig. 2), rendering a reduced FWHM. Compared with LECs based on neat films of $[Ir(dFppy)_2(SB)]^+(PF_6^-)$, which possess broad EL emission (FWHM, ~100 nm), phosphor-sensitized LECs here exhibit much more saturated EL spectra, indicating that such a technique is effective for color tuning and maybe also for achieving more saturated colors by appropriate combinations of phosphorescent hosts and fluorescent guests.

Peak EQEs and peak power efficiencies (at current densities <0.2 mA cm^{-2}) of phosphor-sensitized fluorescent LECs with various R6G doping concentrations are shown in Fig. 7. The device EQE decreases monotonically while the device power efficiency first increases then decreases as the doping concentration increases from 0.05 to 0.2 wt%. Since both devices with 0.05 and 0.1 wt% R6G show similar EQEs and device currents under the same constant bias voltage, a higher power efficiency obtained from the 0.1 wt% R6G-doped device is attributed to better matching between its EL spectrum (Fig. 6) and the luminosity function,[26] which renders higher lumen values of the EL emission. With a R6G doping concentration of 0.05 wt%, the peak EQE (cd A^{-1}) efficiency and power efficiency of the phosphor-sensitized fluorescent LEC reach 5.5%, 19 cd A^{-1} and 21.3 lm W^{-1}, respectively. The achieved EQE of 5.5% is among the highest reported for fluorescent solid-state LECs.[27,28]

The maximal EQE (~5.5%) achieved from R6G-doped phosphor-sensitized LEC is significantly higher than that (~2.5%) one could expect from a typical layered all-fluorescent device with an emission PLQY of ~50% and an optical out-coupling efficiency of ~20%. It confirms efficient phosphor-sensitization of fluorescence in LEC devices, which enables harvesting of host triplet excitons *via* Förster energy transfer[17] from triplet excitons on the phosphor to singlet excitons on the fluorophore.[18,19] However, the maximal EQE obtained is still lower than the value (~10%) one could expect from a typical layered all-phosphorescence device with a similar emission PLQY. Moreover, as the R6G concentration increases from 0.05 to 0.2 wt%, the PLQY of the emissive layer increases (Fig. 3(a)) while the device EL efficiency decreases (Fig. 7). Such phenomena suggest two possible exciton loss mechanisms: Dexter transfer[29] and/or direct carrier trapping to form triplet excitons on guest molecules. Dexter transfer takes place between host triplets and guest triplets when the guest concentration increases, which would degrade the EL efficiency when occurring.[18] Direct carrier trapping results in formation of triplet exctions on guest molecules directly and would degrade device efficiency, as well. Carrier trapping impedes carrier transport and thus lowers the device current under the same bias voltage as doping concentration increases. The energy levels of host and guest molecules shown in the inset of Fig. 8 were estimated by cyclic voltammetry (CV, see the Experimental section for details). The energy-level offsets between host and guest may result in carrier trapping. However, as shown in Fig. 8, the device current density does not show a clear decreasing trend as the R6G doping concentration increases; the difference in currents between different devices is within the experimental errors. Hence, at low doping concentrations (<0.2 wt%), direct carrier trapping perhaps plays a minor role in the degradation of device efficiency and concentration-dependent Dexter transfer may be more dominant in the present host–guest LEC devices. More studies of appropriate host–guest combinations with a suppressed Dexter transfer may be beneficial to further enhancement of device efficiencies of phosphor-sensitized fluorescent solid-state LECs.

Conclusions

In summary, we have reported highly efficient phosphor-sensitized solid-state LECs utilizing a phosphorescent cationic iridium complex $[Ir(dFppy)_2(SB)]^+(PF_6^-)$ as the host and a fluorescent cationic dye R6G as the guest. Photophysical studies show that R6G retains a high PLQY in highly polar media, revealing its suitable use as an emitting guest in an ionic host matrix. Such solid-state LECs achieve quantum efficiency (cd A^{-1}), efficiency, and power efficiency of up to 5.5% photon/electron, 19 cd A^{-1} and 21.3 lm W^{-1}, respectively. The device quantum efficiency observed is among the highest reported for fluorescent LECs and is higher than one would expect from the PLQY of the R6G fluorescent dye in the host film, thus indicating that phosphor-sensitization is useful for achieving highly efficient fluorescent LECs. Moreover, using the narrow-band fluorescent emitters,

such as R6G (FWHM ~50 nm) is effective in improving the color saturation of solid-state LECs based on cationic complexes.

Experimental

The neat films of the host, mixed host–guest films, and guest-dispersed poly(methyl methacrylate) (PMMA) films (~100 nm) for photophysical studies were spin-coated onto quartz substrates using mixed solutions (in acetonitrile (MeCN)) of various ratios. The thicknesses of the spin-coated films was ~100 nm, as measured by ellipsometry. PMMA was used as a nonionic inert matrix for dispersing guest molecules in the comparative studies of photophysical properties in various hosts. Since in LECs, a salt $BMIM^+(PF_6^-)$ of 19 wt% was also added to provide additional mobile ions and to shorten the device response time,[8] photophysical properties of the host–guest-salt three-component system were also characterized. Photophysical characteristics of guests in solutions were collected at room temperature by using 10^{-5} M CH_2Cl_2 and MeOH solutions.

UV-visible absorption spectra were recorded on a spectrophotometer. PL spectra were measured with a cooled charge coupled device (CCD) coupled to a monochromator using the 325 nm line of the He–Cd laser as the excitation. PLQYs for both solution and thin-film samples were determined with a calibrated integrating sphere system.[10] Excited-state lifetimes of samples were measured using the time-correlated single photon counting technique,[10] in which a photomultiplier and a sub-nanosecond pulsed UV laser diode were used as the detector and the pulsed excitation source.[10] The transient PL signals were detected at proper wavelengths selected by the monochromator.

Oxidation and reduction potentials of compounds were determined by CV (scan rate 100 mV s^{-1}) in CH_2Cl_2 or MeCN solutions (1.0 mM). A glassy carbon electrode and a platinum wire were used as the working electrode and the counter electrode, respectively. All potentials were recorded *versus* the Ag/AgCl (saturated) reference electrode. Redox CV was performed using 0.1 M of tetra-*n*-butylammonium hexafluorophosphate ($TBAPF_6$) in CH_2Cl_2 (oxidation) or MeCN (reduction) as the supporting electrolyte. The ferrocenium/ferrocene redox couple in CH_2Cl_2/$TBAPF_6$ and MeCN/$TBAPF_6$ showed $E^{0\prime} = +0.48$ V *versus* Ag/AgCl (saturated).

LEC devices were fabricated by spin-coating the mixed solutions of host, guest and $BMIM^+(PF_6^-)$ (19 wt%) on indium-tin-oxide (ITO) coated glass substrates. ITO-coated glass substrates were cleaned and treated with UV/ozone prior to coating of the emissive layer. The preparation of solutions and spin-coating of thin films (~100 nm) were performed in a nitrogen atmosphere in a glove box. To reduce the turn-on time of the LEC device, the ionic liquid $[BMIM^+(PF_6)^-]$ of 19 wt% was added to enhance the ionic conductivity of thin films.[8] After spin coating, the thin films were then baked at 70 °C, followed by thermal evaporation of a 150 nm Ag top contact in a vacuum chamber (~10^{-6} torr). The EL spectra of the LECs were taken with a calibrated CCD spectrograph. The photocurrents induced by the EL emission of LEC devices were measured using a source-measurement unit and a Si photodiode calibrated with the Photo Research PR-650 spectroradiometer. The EQEs of the LECs were consequently calculated with the responsivity spectrum of the Si photodiode, EL spectra, photocurrents and device currents of the LECs. All device measurements were performed under a constant bias voltage (2.6–2.9 V).

Acknowledgements

The authors gratefully acknowledge financial support from the National Science Council and Ministry of Economic Affairs of Taiwan.

References

1 Q. Pei, G. Yu, C. Zhang, Y. Yang and A. J. Heeger, *Science*, 1995, **269**, 1086.
2 Q. Pei, Y. Yang, G. Yu, C. Zhang and A. J. Heeger, *J. Am. Chem. Soc.*, 1996, **118**, 3922.
3 C. W. Tang and S. A. VanSlyke, *Appl. Phys. Lett.*, 1987, **51**, 913.
4 J. K. Lee, D. S. Yoo, E. S. Handy and M. F. Rubner, *Appl. Phys. Lett.*, 1996, **69**, 1686.
5 C. Y. Liu and A. J. Bard, *J. Am. Chem. Soc.*, 2002, **124**, 4190.
6 J. D. Slinker, A. A. Gorodetsky, M. S. Lowry, J. Wang, S. Parker, R. Rohl, S. Bernhard and G. G. Malliaras, *J. Am. Chem. Soc.*, 2004, **126**, 2763.
7 A. R. Hosseini, C. Y. Koh, J. D. Slinker, S. Flores-Torres, H. D. Abruña and G. G. Malliaras, *Chem. Mater.*, 2005, **17**, 6114.
8 S. T. Parker, J. D. Slinker, M. S. Lowry, M. P. Cox, S. Bernhard and G. G. Malliaras, *Chem. Mater.*, 2005, **17**, 3187.
9 A. B. Tamayo, S. Garon, T. Sajoto, P. I. Djurovich, I. M. Tsyba, R. Bau and M. E. Thompson, *Inorg. Chem.*, 2005, **44**, 8723.
10 H.-C. Su, F.-C. Fang, T.-Y. Hwu, H.-H. Hsieh, H.-F. Chen, G.-H. Lee, S.-M. Peng, K.-T. Wong and C.-C. Wu, *Adv. Funct. Mater.*, 2007, **17**, 1019.
11 H.-C. Su, C.-C. Wu, F.-C. Fang and K.-T. Wong, *Appl. Phys. Lett.*, 2006, **89**, 261118.
12 J. D. Slinker, J. Rivnay, J. S. Moskowitz, J. B. Parker, S. Bernhard, H. D. Abruña and G. G. Malliaras, *J. Mater. Chem.*, 2007, **17**, 2976.
13 H.-C. Su, H.-F. Chen, F.-C. Fang, C.-C. Liu, C.-C. Wu, K.-T. Wong, Y.-H. Liu and S.-M. Peng, *J. Am. Chem. Soc.*, 2008, **130**, 3413.
14 H.-C. Su, H.-F. Chen, C.-C. Wu and K.-T. Wong, *Chem.–Asian J.*, 2008, **3**, 1922.
15 J. Li, P. I. Djurovich, B. D. Alleyne, M. Yousufuddin, N. N. Ho, J. C. Thomas, J. C. Peters, R. Bau and M. E. Thompson, *Inorg. Chem.*, 2005, **44**, 1713.
16 F.-C. Chen, Y. Yang and Q. Pei, *Appl. Phys. Lett.*, 2002, **81**, 4278.
17 T. Förster, *Discuss. Faraday Soc.*, 1959, **27**, 7.
18 M. A. Baldo, M. E. Thompson and S. R. Forrest, *Nature*, 2000, **403**, 750.
19 B. W. D'Andrade, M. A. Baldo, C. Adachi, J. Brooks, M. E. Thompson and S. R. Forrest, *Appl. Phys. Lett.*, 2001, **79**, 1045.
20 V. Bulovic, A. Shoustikov, M. A. Baldo, E. Bose, V. G. Kozlov, M. E. Thompson and S. R. Forrest, *Chem. Phys. Lett.*, 1998, **287**, 455.
21 A. V. Deshpande and E. B. Namdas, *J. Lumin.*, 2000, **91**, 25.
22 G. Kalyuzhny, M. Buda, J. McNeill, P. Barbara and A. J. Bard, *J. Am. Chem. Soc.*, 2003, **125**, 6272.
23 H. J. Bolink, E. Coronado, R. D. Costa, E. Ortí, M. Sessolo, S. Graber, K. Doyle, M. Neuburger, C. E. Housecroft and E. C. Constable, *Adv. Mater.*, 2008, **20**, 3910.
24 S. Graber, K. Doyle, M. Neuburger, C. E. Housecroft, E. C. Constable, R. D. Costa, E. Ortí, D. Repetto and H. J. Bolink, *J. Am. Chem. Soc.*, 2008, **130**, 14944.
25 R. D. Costa, E. Ortí, H. J. Bolink, S. Graber, C. E. Housecroft, M. Neuburger, S. Schaffnerb and E. C. Constable, *Chem. Commun.*, 2009, 2029.
26 G. Wyszecki, and W. S. Stiles, *Color Science - Concepts and Methods, Quantitative Data and Formulae*, Wiley-Interscience, New York, 2nd edn, 2000.
27 G. Yu, Y. Cao, M. Andersson, J. Gao and A. J. Heeger, *Adv. Mater.*, 1998, **10**, 385.
28 Y. Yang and Q. Pei, *J. Appl. Phys.*, 1997, **81**, 3294.
29 D. L. Dexter, *J. Chem. Phys.*, 1953, **21**, 836.

